PHYSICAL REVIEW B, VOLUME 64, 235207

Grazing incidence diffuse x-ray scattering investigation of the properties of irradiation-induced point defects in silicon

P. Partyka,[1] Y. Zhong,[1] K. Nordlund,[1,2] and R. S. Averback[1]
[1]*Department of Materials Science and Engineering, University of Illinois at Urbana-Champaign, Urbana, Illinois*
[2]*Accelerator Laboratory, University of Helsinki, Finland*

I. M. Robinson
Department of Physics, University of Illinois at Urbana-Champaign, Urbana, Illinois

P. Ehrhart
IFF, Forschungszentrum, Jülich, D-52425 Jülich, Germany
(Received 11 June 2001; published 27 November 2001)

Point-defect properties in ion-irradiated Si were investigated using *in situ* grazing incidence diffuse x-ray scattering. Bombardment with 4.5-keV He at 100 K and 3-MeV electrons at 6 K led to the production of Frenkel pairs. These defects are characterized by close-pair configurations and by relaxation volumes of vacancies and interstitials that have nearly the same magnitude, but opposite sign. Thermally activated motion of interstitial atoms occurs above ≈150 K, while that for vacancies occurs above ≈175 K. The motion of interstitials below 150 K during electron irradiation is shown to be induced by electronic excitation, and it is negligible for ion irradiations. Similar results were observed for irradiation with 20-keV Ga and 1.0-MeV Ar, although the defects were already clustered upon bombardment at 100 K. Correlation distances between vacancies and interstitials in cascades are obtained.

DOI: 10.1103/PhysRevB.64.235207 PACS number(s): 61.72.Dd, 61.72.Cc, 61.72.Ji, 61.82.Fk

I. INTRODUCTION

The properties of implantation-induced defects play a fundamental role in the processing of submicron Si-based devices, and indeed much effort has been directed on this subject over the past 30 years.[1–6] Most recently, attention has focused on the interstitial Si atom and interstitial clusters, owing in large part to the problems of transient enhanced diffusion.[6] Despite this enormous past effort, the detailed structure and atomic mobilities of point defects in Si, particularly those of the single self-interstitial atom, remain controversial, and rationalizing the results derived from low-temperature irradiation experiments with diffusion measurements at high temperatures has been a difficult task.[1,7] For example, the activation enthalpies of vacancies vary by factors of 5–10 when deduced from irradiation versus diffusion experiments. For interstitials a similar discrepancy might exist; however, this discrepancy is often not considered in the discussion of diffusion data[7] due to possible contributions of athermal migration during irradiation. Most information about the properties of intrinsic defects in Si, and other covalently bonded materials, has come from spectroscopic methods that probe electronic states in the band gap. Self-interstitial atoms in Si, however, do not give rise to such states, and therefore most of what is known about this defect comes from indirect measurements, or theory. X-ray diffuse scattering offers an alternative, complementary means to probe point defect properties, as it is sensitive to the elastic strain fields around the defects rather than to electronic states. In the present work, we employ this method to examine the mobility and structure of interstitials in Si.

It is now well established from electron paramagnetic resonance (EPR) measurements that some interstitial atoms are mobile during MeV electron irradiation at very low temperatures, $T<10$ K.[1] The introduction rate of these mobile interstitial atoms, however, is only 0.03 cm^{-1} for *p*-type Si and much lower for *n*-type Si. This contrasts dramatically with other work,[5,8] which demonstrated that the total introduction rate of stable defects is ≈1 cm^{-1}. This larger rate corresponds to a reasonable threshold energy of 20–40 eV for defect production. Our ion irradiations yield correspondingly high defect production rates. Hence the fate and the mobility of the majority of defects remain uncertain. Central to answering these questions is whether the interstitial atoms migrate freely by thermal activation at low temperatures or if their motion is stimulated by the extensive electron excitation associated with MeV electron irradiations. Several past studies have examined the influence of electron excitation on stimulated defect motion, see, e.g., Palmer,[9] Lang and Kimerling,[10] and Bourgoin and Corbett.[11] There is an indication of the athermal motion of vacancies; however, the cross section for this process is small so that many isolated vacancies survive irradiation and can be detected by EPR.[1] The question of low-temperature interstitial migration in Si is far less certain, as no signal of the isolated interstitial has been observed. If we assume for the moment that the low-temperature migration of interstitials is indeed stimulated by electronic excitation, as proposed,[1] then there still remains the questions of the temperature at which interstitials do become thermally mobile, and the structures of defects produced by various types of irradiation particle. We will answer these questions by comparing diffuse x-ray scattering (DXS) measurements on Si following 3-MeV electron irradiation with those following 4.5-keV He bombardment, and also by comparing DXS measurements on Si irradiated with different ions, 4.5 keV He, 20-keV Ga, or 1.0-MeV Ar.

Similar to electron irradiation, low-energy He bombardments produce predominantly isolated Frenkel pairs; however, generally overlooked is the fact that the amount of electron excitation per displaced atom is diminished from electron irradiations by more than three orders of magnitude. He irradiations, therefore, make it possible to study the properties of single point defects in virtual absence of electron excitation. Comparison of the defect reactions following MeV electron and low-energy He irradiation thus provides a powerful means to assess the influence of electron excitation, particularly if the same experimental method is employed to probe the defects produced by the two irradiations.

The properties of defects produced in high energy recoil events were examined by using 20-keV Ga and 1.0-MeV Ar irradiations. For these bombardments the electronic excitation is reduced an additional two orders of magnitude relative to their defect production cross sections; however, the defects are no longer produced in isolation, but rather in energetic displacement cascades.[12,13] These irradiations with heavy ions, therefore, made possible an examination of cascade effects on defect reactions and structures.

II. EXPERIMENT

Huang diffuse x-ray scattering is a well-established method for examining the structure of defects in irradiated crystals;[14] however, it has been used almost exclusively with MeV electron and fast neutron irradiations, for which the defects are created homogeneously throughout a thick specimen. For low-energy ion bombardments, such as the 4.5-keV He or 20-keV Ga bombardments of Si employed here, the average depth of the damage, $\langle x \rangle$, is $\approx$50 and $\approx$30 nm, respectively.[15] These depths are much shallower than the penetration depth of x rays. We thus employed a grazing incidence scattering geometry.[16] For the present studies it was necessary to cool the specimens to $\approx$100 K and perform *in situ* bombardments. In addition, ultrahigh-vacuum (UHV) conditions are required to limit condensation of residual gases on the sample surface. We emphasize this point owing to the shallow penetration depth of both the low-energy ions and the glancing x rays in these experiments.

The current experiments were performed at beamline X-16A at the National Synchrotron Light Source,[17] where facilities are available for *in situ* bombardments under the conditions just described. The He irradiations were performed using a 4.5-keV ion source. The beam was broadly rastered to assure a uniform flux over the 0.5×0.5-cm^2 specimen area. The ion flux was measured *in situ* using a Faraday cup that was placed in front of the sample before and after the irradiations. For the Ga irradiations, a UHV liquid-metal ion source was employed. For both types of irradiation, the x-ray scattering was measured prior to irradiation, i.e., the background, and then again following each of a series of dose increments. Another series of experiments was performed using samples that were irradiated *ex situ* with 1-MeV Ar^+ ions. For these experiments, the background scattering was obtained after annealing the samples in the scattering chamber to high temperature. The specimens employed for the ion irradiations were lightly P-doped Czochralski (Cz)-Si(111), with an electrical resistivity of $\approx$100 Ω cm, while both Cz and float zone (FZ) Si samples were employed for the electron irradiations. The experimental procedures for low temperature electron irradiations were described previously (see, e.g., Ref. 18).

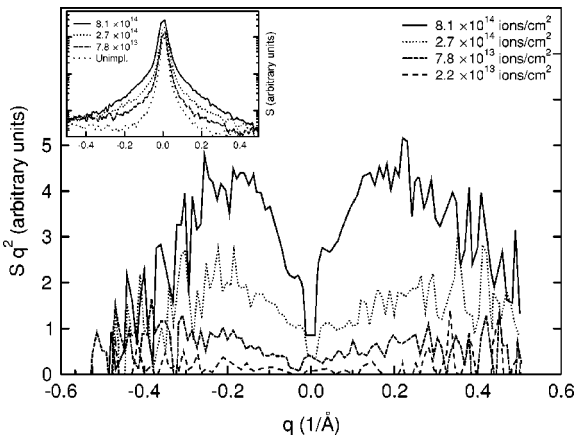

FIG. 1. Diffuse x-ray scattering intensities from defects produced by 4.5-keV He bombardment at 100 K, plotted as Sq^2 vs scattering vector q. Inset are corresponding data plotted as S vs q. S is the total scattering intensity.

III. RESULTS

A. 4.5-keV He vs 3.0-MeV electron damage

Typical scattering intensities near a (220) in-plane reciprocal-lattice point **G**, following bombardment at 100 K with 4.5-keV He from doses of 7.8×10^{13}/cm^2 to 8.1×10^{14}/cm^2, are shown inset in Fig. 1. The defect scattering was obtained by subtracting out the background intensities, which are represented by the curve for zero fluence in the inset. These scattering data are plotted in the main part of Fig. 1 as Sq^2 versus q, where q is the distance in reciprocal space between the scattering vectors **K** and **G**, and the scan is in the radial direction. The product Sq^2, is plotted here since Huang scattering typically scales inversely with q^2.[19] The average scattering intensity (Sq^2) is plotted as a function of dose in Fig. 2, where at 100 K it is seen to increase nearly linearly with the fluence. Corresponding data from electron irradiations are plotted in a similar fashion in Fig. 3, for comparison. Both sets of data reveal strong deviations from the expected q^{-2} dependence, with the product Sq^2 decreasing markedly at small q. Deviations from a q^{-2} dependence generally arise when the scattering centers are spatially correlated. Indeed, similar scattering behavior was observed for electron irradiated GaAs,[18] InP,[20] and Ge.[21] In these studies the deviations were attributed to the spatial correlation between the vacancy and interstitial comprising each Frenkel pair.

The particularly strong reduction in scattering intensity that we observe at small q indicates that the locations of the vacancies and interstitials are also correlated in Si, and that the relaxation volumes of the two defects in Si are of nearly equal magnitude but of opposite sign. This interpretation of the scattering data is affirmed by Fig. 4 where calculated

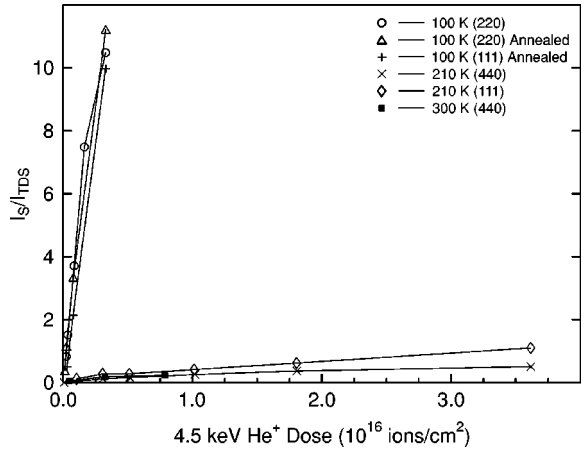

FIG. 2. Ratio of the integral diffuse scattering intensity I, arising from defects to the thermal diffuse background, as a function of dose with 4.5-keV He ions. Results at different reciprocal-lattice vectors and for different irradiation temperatures are shown.

scattering intensities from various defects in Si are plotted as a function of q. The calculations were performed by first using computer simulations to obtain the displacement fields around the defects, and subsequently performing a discrete sum for the scattering intensity. The details of our calculation procedures are found in Ref. 22. It is noteworthy that the reduced scattering at small q observed here for Si and other semiconductors is not found in metals; this is simply a consequence of the relaxation volumes of interstitials in metals being much greater than those of vacancies.[23] Measurements of the lattice parameter of Si showed no measurable changes ($\Delta a/a \leqslant 0.05$ per atom fraction of Frenkel pairs) during electron irradiation and thus directly corroborate the relative relaxation volumes deduced from the DXS measurements.

Since the reduced scattering at small q arises from the correlation between the vacancy and interstitial positions, the correlation distance could be obtained by comparing our ex-

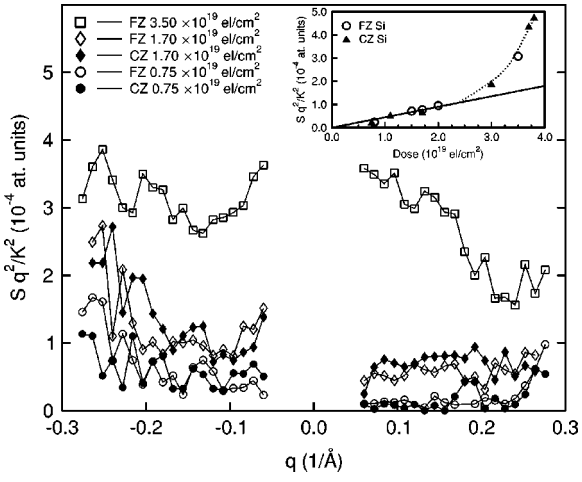

FIG. 3. Diffuse x-ray scattering intensities from irradiation-induced defects plotted as Sq^2 vs scattering vector q due to 3.0-MeV electron irradiation at 4.6 K. Inset are average values plotted as a function of dose. K is the magnitude of the reciprocal lattice vector.

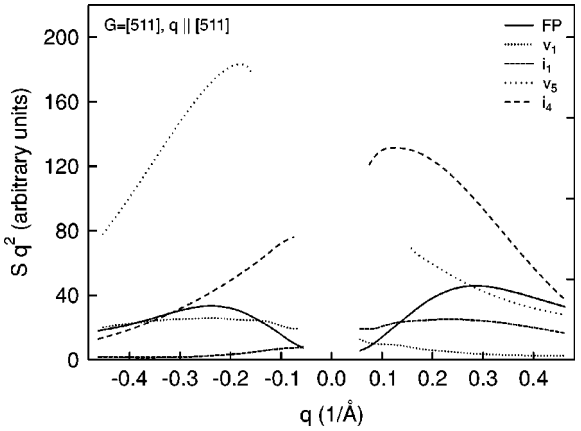

FIG. 4. Scattering intensities calculated for various defects using computer simulations. See Ref. 22 for details.

perimental data with results of the simulations. From data like that shown in Figs. 1 and 3, we obtain separation distances of ≈0.8 and ≈1.2 nm for the electron and He ion irradiations, respectively, when irradiated to low doses. These values agree well with molecular-dynamics simulations of Frenkel pair production in low energy recoil events,[24,25] and thus provide an important validation test of our DXS simulations and the interpretations of the data that follow. For example, also shown in Fig. 4 are the scattering intensities from both isolated vacancies and isolated interstitials. Note that since the relaxation volumes have nearly the same magnitude but are of opposite sign, the scattering intensities have nearly the same magnitude but are far stronger on one side of the Bragg peak, or the other (positive q for interstitials and negative q for vacancies). This qualitative result is also obtained from calculations of Huang scattering from idealized defect structures based on elasticity theory.[19] Asymmetries in the scattering, therefore, provide specific information about the structure of each of the two defects. Scattering intensities from small defect clusters are also shown in Fig. 4, and it is seen that they are approximately proportional to the square of the number of defects in the cluster. This indicates that the strain fields arising from the defects in the clusters superpose linearly.

In comparing our electron and ion irradiation results, we note that the strong suppression of scattering intensities at small q is observed for electron irradiations only for the samples irradiated to low fluence, $<2\times10^{19}\,e^-/\mathrm{cm}^2$ (see Fig. 3), while it is observed after all He ion irradiations (Fig. 1). Unfortunately we cannot directly compare the defect concentrations produced by the two types of irradiations, since we did not measure the absolute x-ray scattering intensities for the ion irradiations. Normalization of the two sets of data to the thermal diffuse background, however, enables an estimation of the relative defect concentrations. This procedure indicates that the Frenkel pair concentration for the lowest ion fluence (≈0.001 displacements per atom based on a Kinchin-Pease model[15]) is approximately equal to that for the highest electron fluence. This estimate agrees well with defect production calculations.

Since the close-pair correlation vanishes for the electron irradiation at high dose, we computed the average scattering

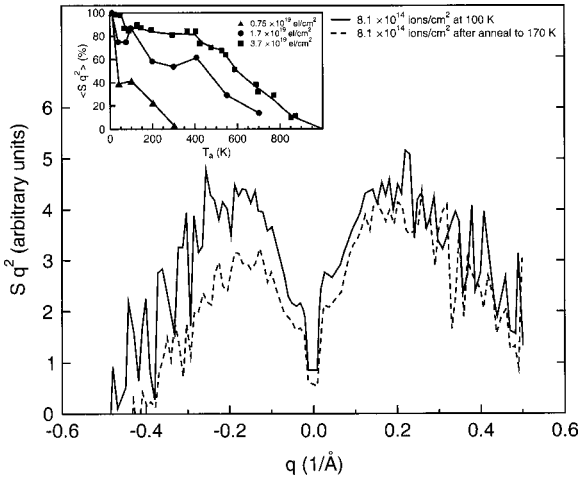

FIG. 5. Diffuse scattering intensities after irradiation with 4.5-keV He at 100 K, and again after annealing to 170 K. Inset is the fractional recovery of diffuse scattering from defects produced by −3-MeV electrons as a function of annealing temperature.

$\langle Sq^2 \rangle$ for the different electron irradiations and plotted them versus the dose, as shown inset in Fig. 3. It is noteworthy that the dose where the vacancy-interstitial correlation is lost during electron irradiation, $\approx 3.5 \times 10^{19}/\mathrm{cm}^2$, the integral scattering intensity begins to deviate from a linear dose dependence, becoming supralinear. This deviation signals that interstitials are no longer correlated with their vacancies, but rather are clustered. For the ion irradiations, the linear—and finally sublinear—dependence of the average intensity persists to a dose nearly two orders of magnitude higher than after the highest electron dose; see Fig. 2. Some small changes in the distribution of scattering intensity are observed for the He irradiations at very high doses; these will be discussed below, along with the data for the Ga^+ and Ar^+ implantations.

B. Low-temperature annealing

We have also examined the annealing of the damage produced in Si following bombardment at low temperatures. Some annealing, ≈20% occurs between 4.6 and 100 K following electron irradiation to any dose, as seen inset in Fig. 5; we attribute this to close-pair recovery. Above 100 K, additional annealing was observed between 100 and 200 K for the samples irradiated to low dose, while essentially no additional annealing of the symmetrical part of the scattering was observed between 100 and 500 K following the high dose treatment. The He bombardments were performed at 100 or 120 K, and consequently any possible close-pair annealing at very low temperatures could not be examined. A significant amount of recovery was observed between 100 and 170 K, as shown in Fig. 5. Defect annealing is recognized by the decrease in scattering intensity at negative q, but with correspondingly little or no change at positive q. The fractional recovery during this annealing step was nearly independent of the amount of damage introduced at 100 or 120 K. We can estimate the recovery from data like that shown in Fig. 5 by assuming that vacancies are not mobile during this annealing interval, an assumption that we justify below. In this case, the percentage reduction in intensity at negative q, which derives mostly from the loss of vacancies, is linearly proportional to the fractional recovery. The recovery is ≈35%, which is very similar to that found after the low dose electron irradiations. Noteworthy is that stage-I recovery in metals following He bombardment to comparable doses is also ≈35%.[26]

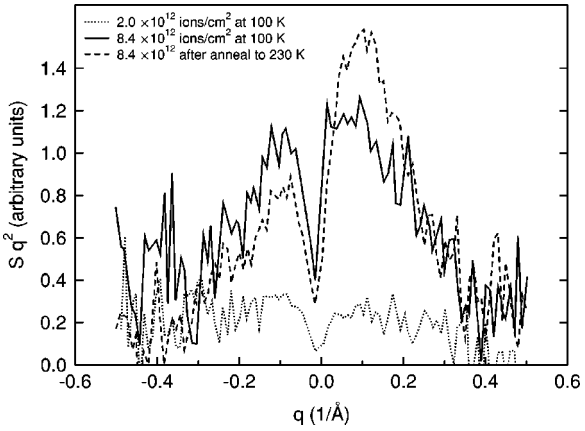

FIG. 6. Diffuse scattering intensities after irradiation with 20-keV Ga at 100 K, and again after annealing to 230 K.

C. Heavy-ion irradiations

Results for 20-keV Ga^+ bombardment of Si at 100 K are shown in Fig. 6. For Ga, the ratio of damage energy to electron excitation is reduced an additional factor of 10^2. The scattering data reveal a similar spatial correlation between vacancy and interstitial defects, despite their being produced in energetic displacement cascades. The annealing behavior is also quite similar, as illustrated in Fig. 6. Again it is observed that the scattering at positive q becomes significantly larger than the contribution at negative q after annealing at 100 K. For the irradiation represented here, the scattering at positive q actually increases on annealing, providing convincing evidence that this is indeed an interstitial clustering reaction. There are other differences in the scattering for the He and Ga ion irradiations as well. Most notable is the distribution of scattering intensities for the two irradiations. At low doses, the products Sq^2, plotted in Figs. 1 and 6, begin to decrease near the Bragg peak at different values of $q = q^*$. For the low dose He irradiations, q^* is ≈0.20 $\mathrm{Å}^{-1}$, decreasing to ≈0.10 $\mathrm{Å}^{-1}$ at the highest doses. For the Ga irradiations, $q^* \approx 0.05\,\mathrm{Å}^{-1}$ at low dose (2×10^{12} Ga ions cm^{-2}), and ≈0.025 $\mathrm{Å}^{-1}$ at high dose (8.4×10^{12} Ga ions cm^{-2}). These different values of q^* illustrate the different correlation distances between vacancies and interstitials and hence quite different defect structures for the two types of irradiations.

D. Irradiations at elevated temperatures

Diffuse x-ray scattering measurements were also performed following irradiation at elevated temperatures. For He, the irradiations were performed at 120, 220, and 300 K,

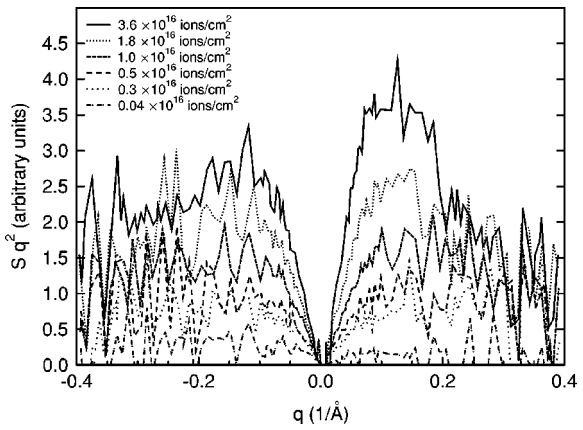

FIG. 7. Diffuse scattering intensities due to 4.5-keV He irradiation at 220 K for various ion doses.

in addition to 100 K, while for the Ga ions the additional irradiations were performed at 150, 220, and 300 K. Typical data sets are illustrated in Fig. 7 (He at 220 K) and Fig. 8 (Ga at 150 K). For He bombardments at 220 K, the results are quite different from both the Ga irradiation at 150 K and the He irradiations at 100 K followed by anneal to 170 K. For doses below $0.5\times10^{16}\,\mathrm{cm}^{-2}$, the scattering has become nearly symmetric. Analysis of the data shows, in fact, that the average scattering $\langle Sq^2\rangle$ is somewhat stronger at negative q at these lower doses. At higher doses, the trend reverses and the scattering becomes stronger at positive q, as seen in Fig. 7. Spatial correlations between vacancies and interstitials are again observed for both types of irradiation by the reduction in Sq^2 at small q. For the He irradiation, q^* decreases to ≈0.075 Å^{-1}, while for the Ga irradiation q^* remains at ≈0.05 Å^{-1}.

Finally, we have performed irradiations with 1-MeV Ar over a wide range of temperatures. These irradiations were performed *ex situ* using a 3.0-MeV Van de Graaff accelerator. In this case the specimens were warmed to room temperature prior to the x-ray measurements at 300 K; therefore, some annealing takes place prior to examination. Nevertheless, these data allow for some direct conclusions on the defect mobility. Our data from specimens irradiated at 100 K

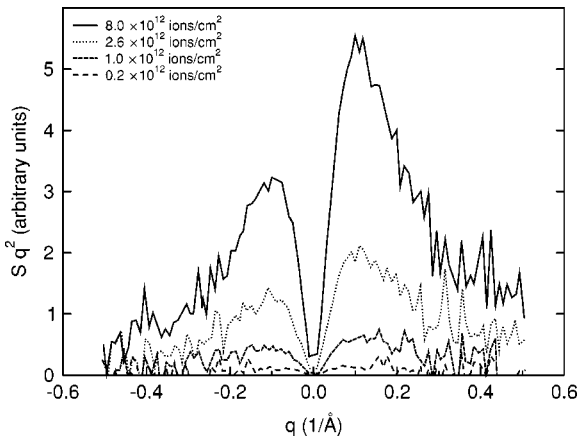

FIG. 8. Diffuse scattering intensities due to 20-keV Ga irradiation at 150 K for various ion doses.

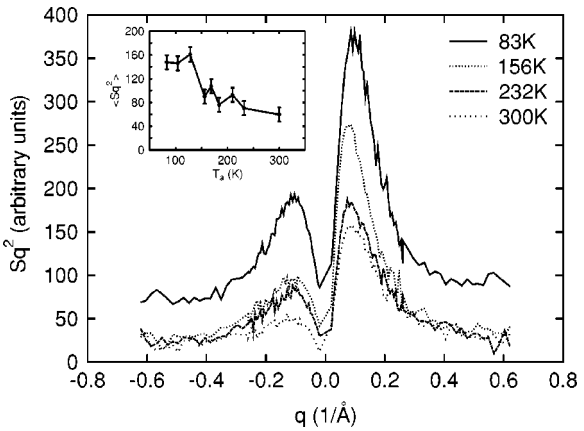

FIG. 9. Diffuse scattering intensities following 1.0-MeV Ar irradiation at specified temperatures followed by warming to room temperature. Inset are the integral scattering intensities as a function of irradiation temperature.

with either He or Ga, and then warmed to room temperature, showed that the reduction in scattering intensity was less than a factor of ≈2. The reduction in intensity for specimens irradiated at 300 K with these same ions, on the other hand, was reduced by two orders of magnitude (see Fig. 2). It is indeed generally found that recovery during irradiation at elevated temperatures far exceeds that for annealing to the same temperature following low-temperature irradiation. The ratio of this difference, however, depends on the dose, being the largest at high doses. It is therefore often possible to find the temperature at which defects become mobile by irradiating specimens at various temperatures below room temperature and subsequently analyzing them at room temperature. Data obtained using this procedure are shown in Fig. 9. The main portion of Fig. 9 shows that the scattering following the Ar irradiation conforms to the same pattern as before, with the scattering being somewhat larger at positive q. We analyzed the data for total defect concentrations by obtaining $\langle Sq^2\rangle$; these results are inset in this same figure. Here it is observed that the scattering intensity is constant to within the experimental uncertainty below $T\approx150\,\mathrm{K}$, and then decreases by a factor of ≈2. The scattering then decreases slowly as the irradiation temperature is further increased.

IV. DISCUSSION

A. Athermal mobility of interstitials

We begin the discussion of point defect reactions in irradiated Si by considering the mobility of interstitials at $T<6\,\mathrm{K}$ during MeV electron irradiation. Our comparative x-ray scattering results from 4.5-keV He and 3-MeV electron irradiations strongly support the hypothesis that the motion of interstitial atoms at low temperatures is stimulated by electronic excitation. This is indicated, first, by the loss at high fluences of the correlation between the vacancy-interstitial positions observed during electron irradiation at low fluences. At least one of the defects, presumably the interstitial, migrates during prolonged irradiation and either recombines with its nearby vacancy partner or simply mi-

grates from it. Note that since the concentration of Frenkel pairs for the largest electron doses is at most $\approx 10^{-3}$, the distance between randomly located interstitials and vacancies is greater than ≈ 3 nm. The value of q^* for this correlation distance, ≈ 0.05 Å^{-1}, was too close to the Bragg peak to observe in these experiments; see Fig. 3. The loss of correlation cannot be attributed to a higher defect concentration *per se*, since the close-pair correlation is retained at far higher defect levels when they are introduced during 4.5-keV He^+ bombardments or even 20-keV Ga^+ bombardment.

Additional evidence that interstitials have undergone stimulated migration during prolonged electron irradiation derives from the annealing behavior between 100 and 400 K. Annealing is observed in this temperature regime after electron irradiation to low doses, i.e., where the close-pair correlation still persists, and for both the He and Ga irradiations to any dose. No annealing is observed in this temperature interval, however, following electron irradiation to high doses. This implies that interstitial atoms migrate during prolonged electron irradiation, and form immobile defect clusters (such as a di-interstitial). Trapping at impurities (such as oxygen) can be neglected owing to the high defect concentrations. This latter conclusion is experimentally supported in this work by the identical behavior of electron irradiated Cz- and FZ-grown Si, the recovery at low electron dose, and the recovery observed for all ion irradiations.

B. Thermally activated interstitial mobility

Since the low-temperature migration of Si interstitials can now be safely attributed to electronic stimulation, we turn to the question of the onset temperature for thermally activated migration of the interstitials. For the He ion irradiations, it is observed that during annealing to ≈ 170 K, the scattering intensity at positive q increases relative to that at negative q. This is also observed for the Ga irradiations, although for Ga the first annealing temperature is 230 K. Since the scattering at positive q values derives mostly from interstitial defects, the data are interpreted straightforwardly by assuming that interstitials become mobile between 120 and 170 K, and that they either recombine with vacancies or form immobile di-interstitial clusters. Recombination leads to a reduced number of vacancies and a decrease in scattering at negative q, while the corresponding decrease in the number of interstitials is nearly compensated for in the scattering at positive q by the increased scattering from defects in the form of clusters, (see Fig. 4). The formation of only small clusters with an average size containing ≈ 2 defects implies that the di-interstitial is immobile below room temperature. If larger clusters were present, the asymmetry in the scattering would be larger than that shown in Fig. 1. The assumption of an immobile di-interstitial is additionally supported by the attribution of the classical P6 EPR spectrum to the di-interstitial, as this defect is stable up to 400 K.[3]

The Ar irradiations establish the onset temperature for the thermally activated motion of interstitials more precisely. As seen in Fig. 9, the retained damage after annealing to room temperature drops by a factor of 2 when the irradiation temperature increases above ≈ 150 K. The reason for the reduced damage at 150 K has simple kinetic origins. At low defect concentrations, mobile interstitials (or vacancies) have a high probability to find their close pair partner and recombine. If the defect (e.g., interstitial) avoids annihilation with its partner, however, it gains roughly an equal chance of forming a cluster with another interstitial as of finding another vacancy and recombining. Irradiation above the temperature at which one defect becomes mobile, T_m, typically leads to this low concentration situation, because recovery is occurring during the irradiation. Irradiation at temperatures below T_m, on the other hand, allows defect concentrations to build up during irradiation. For the defect concentrations used in the present Ar irradiation experiments, the distances between defects were comparable to the distances between close pairs, so that defects gain equal chance of recombining or clustering. Consequently, the large amount of correlated recovery observed at high temperatures is lost for irradiation at low temperatures to high defect concentrations. The vacancies may also become mobile during the annealing to 300 K in this experiment, but while this may complicate the kinetics somewhat, the same basic argument for larger defect retention for irradiations below 150 K is applicable. With reasonable assumptions on the pre-exponential factors, this migration temperature of 150 K corresponds to an activation energy of 0.3 eV. It is noteworthy that this value, which is unquestionably thermally activated and not ionization induced, is much lower than the value of 1.4–1.8 eV deduced from diffusion experiments.[7,27]

C. Vacancy mobility

The onset temperature for vacancy migration is less clearly defined by these experiments, but it appears to lie between 170 and 210 K. The most direct evidence of vacancy motion in these experiments derives from the DXS scattering patterns observed following the 4.5-keV He irradiations at 210 K. At the lowest few doses, but still high relative to the doses at 100 K, the scattering at negative q is very similar to that at positive q (see Fig. 7), indicating that the degree of clustering for vacancies is similar to that for interstitials. At higher doses, the scattering at positive q becomes somewhat larger, but at these doses, $>1 \times 10^{16}\,\mathrm{cm}^{-1}$, the defect clusters can grow much larger than just simple divacancies and di-interstitials, and consequently the relaxations around the defects may become complex.

Other results are also suggestive of vacancy motion in this temperature interval. Note in Fig. 2, for example, that the defect production rate for the 4.5-keV He irradiations drops by nearly a factor of 100 between 100 and 210 K, but without much additional change when irradiated at 300 K. Presumably the large change at 210 K is a consequence of both the vacancy and interstitial being mobile, while the lack of an additional reduction at 300 K is a consequence of no additional defect becoming mobile, i.e., both di-interstitials and divacancies become mobile only at temperatures higher than 300 K. In contrast, the production rate for the 20-keV Ga irradiation changes by only a factor of 2 between 100 and 150 K, but then it drops dramatically at 210 K. Again, no significant additional change is observed at 300 K. Our indi-

cations of vacancy motion in this regime, moreover, appear to be in agreement with earlier results of Watkins. This work yielded migration energies near 0.45 eV to the vacancies with charge states likely to be relevant in the current experiments.[1] The $V^{=}$ charge state of the vacancy with a migration energy of 0.18 eV can be reasonably excluded here, since the Fermi level after high dose irradiations is located not too far from midgap; see Ref. 1 for details. Similar to the condition for the interstitial atom, we note a large difference in the migration temperature of vacancies found here compared to that deduced from diffusion data. For vacancies, however, this difference was recognized earlier, and models for the explanation were proposed, although no general agreement yet exists.

D. Defect structure

Finally we discuss the structure of the defects. As indicated above, the distance separating the vacancy and interstitial is ≈0.8 nm for electron irradiation, and somewhat larger for the 4.5-keV He irradiation, ≈1.2 nm. These distances were determined by computer simulation, which show that the correlation distance of defects scales with $1/q$ in reciprocal space, as expected from analytical theory.[19] It was also noted that the value of q^* for the He irradiations decreased at the highest doses, $\approx 1\times 10^{-15}\,\mathrm{cm}^{-1}$, and that the asymmetry in the scattering increased (more intensity at positive q). This general behavior is expected since the defects begin to overlap at high doses resulting in ''spontaneous'' recombination and clustering. Recombination results in the annihilation of the original population of close-pair defects, which have a small separation, and the creation of an average correlation distance given approximately by the instantaneous concentration. When spontaneous recombination becomes important, q^* should decrease with increasing dose, as observed here. Similarly, when the irradiations are performed at 210 K, the defects are mobile and the original close-pair correlation is again lost.

The observation of small values of q^* for the Ga^+ bombardments appears to have a similar origin. Ga irradiation produces energetic displacement cascades, for which the defects are produced in high concentrations within a single event. Consequently, locally high concentrations of defects are produced even before the cascades begin to overlap, and close-pair defects are eliminated, as discussed for high dose He irradiation. In addition, defect motion within the cascade is stimulated by thermal spikes, and this further contributes to the annihilation of close pair defects. A more detailed analysis of the cascade structure is not yet possible, since it is believed that small amorphous zones may also exist within the cascade region, and we have not yet evaluated with our simulation model how they might contribute to the scattering, if at all for these irradiations. The difficulties of such calculations are the large size of the cascades and the large number of events required for statistical significance.

V. CONCLUSIONS

Our experiments show, first, that the very low-temperature migration of interstitials during electron irradiation is indeed driven by electronic excitation, and that such motion is negligible during ion irradiation. Our experiments further show that interstitial atoms produced by ion irradiation become mobile near 150 K, which means that the activation energy for interstitial migration of ≈0.3 eV is much less than that deduced from thermal diffusion experiments (1.4–1.8 eV).[7,27] Our findings for the migration of vacancies appear to be in agreement with the results summarized by Watkins,[1] viz. vacancies become mobile at ≈175 K. This result is significant in that it confirms, by completely separate means, the far higher mobilities of vacancies obtained by spectroscopic methods (0.32–0.45 eV) than from measurements of thermal diffusion (1.8 eV).[27] As we have established a similar behavior of interstitials and vacancies, our combined results indicate a very general defect behavior in Si, and no longer a peculiarity specific to vacancies. Such a behavior was previously considered by Seeger and Chik in an early attempt to describe all defect properties[28] in terms of an entropy-driven change of the structure of interstitials and vacancies from a localized point defect at low temperatures to an extended configuration at high temperature. Additional theoretical work seems necessary, however, before the high-temperature defects are completely understood. The results on the defect mobilities have obvious consequences for modeling diffusion characteristics following ion implantation, since in this situation the activation enthalpy for defect migration rather than the activation energy for diffusion is the relevant quantity.

Our combined measurements of diffuse x-ray scattering and change in lattice parameter reveal that the relaxation volumes of isolated vacancies and interstitials are of nearly equal magnitudes, but opposite in sign. This result, which is of direct importance for understanding point-defect reactions, has additional significance as a reference mark for *ab initio* calculations of defect structures in Si. These same results also show that the separations of vacancy-interstitial pairs produced in low-energy recoil events are predominantly ≈1 nm, while, for defects produced in cascades, the average distances separating interstitial-vacancy pairs is about twice that distance.

ACKNOWLEDGMENTS

The research was supported by the U.S. National Science Foundation, under Grant No. DMR-9986160 and the U.S. Department of Energy Basic Energy Sciences under Grant No. DEFG02-96-ER45439.

[1] See, e.g., G. D. Watkins, in *Electronic Structure and Properties of Semiconductors*, edited by W. Schroeter, *Materials Science and Technology* Vol. 4 (VCH, Weinheim, 1992), p. 105, and references therein.

[2] J. L. Benton, K. Halliburton, S. Libertino, S. J. Eaglesham, and S. Coffa, J. Appl. Phys. **84**, 4749 (1998).

[3] Y. H. Lee, Appl. Phys. Lett. **73**, 1119 (1997).

[4] N. E. B. Cowern, G. Mannino, P. A. Stolk, F. Roozeboom, H. G.

A. Huizing, J. G. M. van Berkum, F. Cristiano, A. Claverie, and M. Jaraiz, Phys. Rev. Lett. **82**, 4460 (1999).
[5] P. Ehrhart and H. Zillgen, in *Defects and Diffusion in Silicon Processing*, edited by T. Diazade by Rubia, S. Cutta, and P. A. Stolk and C. S. Rafferty, MRS Symposia Proceeding No. 469 (Materials Research Society, Pittsburgh, 1997), p. 175.
[6] D. J. Eaglesham, P. A. Stolk, H.-J. Gossmann, and J. M. Poate, Appl. Phys. Lett. **65**, 2305 (1994).
[7] H. Bracht, MRS Bull. **25**, 22 (2000).
[8] G. Fritsch and J. S. Koehler, Phys. Rev. B **23**, 1859 (1981).
[9] D. W. Palmer, in *Lattice Defects in Semiconductors*, edited by N. B. Urli and J. W. Corbett, Inst. Phys. Conf. Ser. No. 31 (Institute of Physics and Physical Society, London, 1977), p. 144.
[10] D. V. Lang and L. C. Kimerling, Phys. Rev. Lett. **33**, 489 (1976).
[11] J. C. Bourgoin and J. W. Corbett, in *Lattice Defects in Semiconductors*, Inst. Phys. Conf. Ser No. 23 (Institute of Physics and Physical Society, London, 1975), p. 149.
[12] See, e.g., R. S. Averback and T. Diaz de la Rubia, in *Solid State Physics*, edited by H. Ehrenreich and F. Spaepen (Academic Press, New York, 1998), p. 281.
[13] See, e.g., T. Diaz de la Rubia and G. H. Gilmer, Phys. Rev. Lett. **74**, 2507 (1995).
[14] P. Ehrhart, J. Nucl. Mater. **216**, 170 (1994).
[15] SRIM 2000 computer code; see J. Ziegler, J. P. Biersack, and U. Littmark, *Stopping and Range of Ions in Solids* (Pergamon, New York, 1985), Vol. 1.
[16] S. Grotehans, G. Wallner, E. Burkel, H. Metzger, H. Peisl, and H. Wagner, Phys. Rev. B **39**, 8450 (1989).
[17] I. K. Robinson, Acta Crystallogr: Found Crystall. A **54**, 772 (1998).
[18] A. Pillukat and P. Ehrhart, Phys. Rev. B **53**, 7823 (1996).
[19] See, e.g., P. H. Dederichs, J. Phys. F: Met. Phys. **3**, 471 (1973).
[20] K. Karsten and P. Ehrhart, Phys. Rev. B **51**, 10 508 (1995).
[21] P. Ehrhart and H. Zillgen, J. Appl. Phys. **85**, 3503 (1999).
[22] K. Nordlund, P. Partyka, R. S. Averback, I. K. Robinson, and P. Ehrhart, J. Appl. Phys. **88**, 2278 (2000).
[23] P. Ehrhart and H. Schulz in *Properties and Interactions of Atomic Defects in Metals and Alloys. Atomic Defects in Metals*, edited by H. Ullmaier, Landolt-Börnstein, New Series, Group III, Vol. 25 (Springer-Verlag, Berlin, 1991), pp. 88–379.
[24] M. Sayed, J. H. Jefferson, A. B. Walker, and A. G. Cullis, Nucl. Instrum. Methods Phys. Res. B **102**, 232 (1995).
[25] M. J. Caturla, T. Diaz de la Rubia, and G. H. Gilmer, in *Materials Synthesis and Processing Using Ion Beams*, edited by R. J. Culbertson, O. W. Holland, K. S. Jones, and K. Maex, MRS Symposia Proceedings No. 316 (Materials Research Society, Pittsburgh, 1978), p. 704.
[26] See, e.g., R. S. Averback, L. J. Thompson, and K. L. Merkle, J. Nucl. Mater. **69/70**, 714 (1978).
[27] H. Bracht, N. A. Stolwijk, and H. Mehrer, Phys. Rev. B **52**, 16 542 (1995).
[28] A. Seeger and K. P. Chik, Phys. Status Solidi **29**, 455 (1968).